



**AIAA 96-
OVERVIEW OF JAPANESE ELECTRIC
PROPULSION ACTIVITIES**

Kimiya Komurasaki
Nagoya university
Nagoya, Japan

**32nd AIAA/ASME/SAE/ASEE
Joint Propulsion Conference
July 1-3, 1996 / Lake Buena Vista, FL**

OVERVIEW OF JAPANESE ELECTRIC PROPULSION ACTIVITIES

Kimiya Komurasaki*
Nagoya university, Nagoya, Japan

Abstract

Current electric propulsion activities in Japan are reviewed. NASDA completed the thrusting test of the 25 mN ion engine on ETS-VI. The results have been reflected in next ion engine design for COMETS (launch in 1997) ISAS proposed the microwave discharge ion engine as a primary propulsion for the Nereus sampling mission, (launch in 2002) and conducted 300 hours operation test so far. The 150 mN ion engine is under development with the cooperation of NAL, NASDA and companies. On-orbit test of MPD arcjet system, EPEX, by ISAS has been successfully finished on January 1996 with over 40,000 firings. Fundamental experiments and computations on EP and the associated plasma dynamics have been continued for the study of ion thrusters, Hall thrusters, DC arcjets, MPD arcjets and the non-propulsive applications by universities, industries and governmental research institutes.

Introduction

Japan covers a variety of research and development activities in the field of electric propulsion from fundamental studies to in-flight experiments. The ion-propulsion system has been studied and developed by National Space Development Agency of Japan (NASDA), the National Aerospace Laboratory (NAL),¹⁻⁶ Institute of Space and Astronautical Science (ISAS), Mitsubishi Electric Corporation, Toshiba Corporation,⁷⁻⁹ Tokyo Metropolitan Institute of Technology¹⁰⁻¹⁴ and some other organizations. The flight test on ETS-VI is successfully completed. The engines for the COMETS satellite and for Nereus sampling mission are under development. The MPD and arcjet thrusters have been studied by ISAS,¹⁵⁻¹⁹ Ishikawajima-Harima Heavy Industries, Osaka university,²⁰⁻²⁷ Kyushu university,²⁸⁻³¹ Tohoku university,³² and some other universities. In the EPEX on SFU, the MPD arcjet system functioned successfully. It was retrieved by a space shuttle on January 1996. Hall thruster has been studied by University of Tokyo³³ and Nagoya university.³⁴⁻³⁶ Mission analysis has been conducted by University of Tokyo³⁷ and some other organizations. Details are described in the reference papers.

Ion propulsion

Institute of Space and Astronautical Science (ISAS)

ISAS has just started the space program of MUSES-C (Mu-rocket Science and Engineering Satellite). A spacecraft of 360 kg will be launched by a Japanese Mu-5 rocket on January 2002, will rendezvous with Nereus, and bring rocks or sand back to Earth by a reentry capsule. The space propulsion department of ISAS proposes that the space program applies cathode-less microwave discharge ion engines with the ion sources and neutralizers driven by microwave power. Plasma in both the ion source and the neutralizer are generated by the mechanism of electron cyclotron resonance on a 4 GHz microwave. This system is expected to have long life because it is released from degradation of thermionic material and mechanical fatigue due to thermal shock.

In 1994-95, the microwave discharge ion engine including the neutralizer was subjected to a long term operation of 300 hours. In addition, an endurance test of the microwave discharge neutralizer was executed for 1,000 hours

successfully. A three grid system made of carbon-carbon composite material was assembled its mechanical capability was tested. Each grid had a resonate frequency of around 300 Hz. They survived a random vibration environment ten times larger than that of the Mu-rocket.

A large space chamber 2 m diameter and 5 m long has just been constructed, with four cryogenic pumps installed for the real time endurance test (see Fig. 1). A refrigerator will keep the internal surface below -30 °C. Two independent air locks with liner actuators are also installed to insert sensors into the ion beam. The endurance test will be started soon. The computer-aided design and evaluation, as well as the real time endurance test on the ground will contribute to the development of the ion thruster system.

The numerical simulation code on the geometrical change of the acceleration grid was developed by directing our attention to the sputtering by the charge-exchange ions. The code was correlated with the accelerated wear test in which a grid system made of brass was tested for 400 hours under the environment of high neutral gas density. The brass shows a high sputtering rate. The high pressure of the background generates a large amount of the charge exchange ions. The 400 hours in the accelerated wear test is equivalent to several tens of thousands of hours in the real time test using the carbon-carbon composite material on the geometry change of the acceleration grid. The numerical code agreed closely with the results of the accelerated wear test. The tuned numerical code represents the endurance of the carbon-carbon acceleration grid for over one hundred thousand hours. Figure 2 represents one of the numerical results.



Fig. 1 Endurance test facility

* Assistant professor, Member AIAA

Copyright © 1996 by American Institute of Aeronautics and Astronautics, Inc. All right reserved.

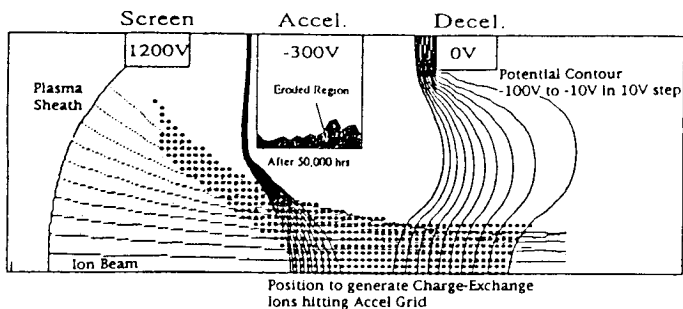


Fig. 2 Numerical simulation on geometry change of the acceleration grid

National Space Development Agency of Japan (NASDA)

NASDA has developed a 25 mN ion engine system (IES) and on-board the Engineering Test Satellite VI (ETS-VI) for its north-south station keeping (NSSK), which was launched in 1994. Because of the failure in reaching the geostationary orbit, NSSK of ETS-VI was not required, therefore IES has been operated as one of on-orbit experiment equipment. NASDA has completed IES beam thrusting after totally 80 hours operation.

The same IES is on-board the Communications and Broadcasting Engineering Test Satellite (COMETS) for its NSSK, which is scheduled to be launched in 1997. Through the operation of ETS-VI on orbit, some design changes were required and reflected in the COMETS IES.

NASDA continues research of large ion thrusters with the National Aerospace Laboratory. The nominal thrust is 150 mN. MELCO and Toshiba join this research. Some application concepts of this large ion thrusters also are under consideration.

An improvement of a 25 mN IES also has been started. The purpose of the research is to simplify the IES function and its operation, to achieve higher performance, to improve reliability, and to reduce its cost.

National Aerospace Laboratory (NAL)

Thrust Measurement A direct thrust measurement of a xenon ion thruster was accomplished by means of a thrust stand.¹ The objectives of this research are to establish thrust measurement technique with high accuracy, to provide accurate thrust values, and to demonstrate coincidence of thrust values both in direct measurement and calculation.

The thrust stand used in this research is of pendulum type (Fig. 3). The thruster is placed on the pendulum. The pendulum has a one-meter-long rigid arm, and supported by a sharp knife edge bearing. Displacement of the pendulum caused by the thrust is measured with a laser displacement meter. Before this measurement, the relation between the displacement and the force applied to the pendulum was obtained by careful calibration. Also after the measurement, this calibration was conducted again to confirm that the displacement-to-force relation would not change. In fact, the pendulum equilibrium position was drifted during the thrust measurement. However, this effect was very small for the time spent to obtain each thrust value.

The thruster submitted to this measurement is a ring-cusp xenon ion thruster.² It has an ion-beam exhausting diameter of 14 cm, and exhausts an ion beam of 480 mA to produce a thrust of 25 mN at a specific impulse of 3,500 s.

The thrust was approximately linear to the beam current

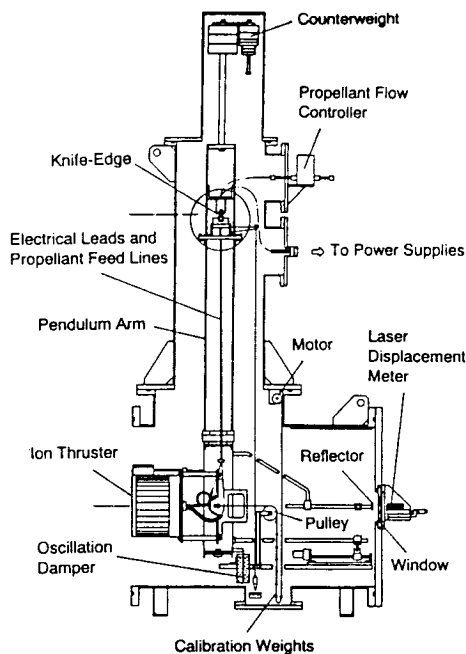


Fig. 3 Cross sectional view of the thrust stand.

and the square root of the beam voltage. Increasing the accelerator grid voltage caused small decreases in the thrust, indicating increasing ion-beam divergence. The probable error in the measured thrust was estimated at about 1%, indicating high accuracy of this measurement.

Thrust values were calculated from the beam current and beam voltage with corrections due to ion-beam divergence and doubly-charged ions. Data for the ion-beam divergence was obtained by traversing a Faraday cup probe through the ion beam.³ The ratio of doubly-to-singly charged ions was estimated from the former data in the same thruster. The calculated thrust values were in good agreements with the measured values, and the difference was only about 3%.

Study on Ion-Beam Structures Ion-beamlet structures were studied experimentally.⁴ It is known from the shapes of accelerator grid holes after wear tests that ion-beamlet profiles can be distorted to hexagonal shape even when grid holes are circular. The objective of this study is to understand the mechanism of this beamlet distortion.

A single beamlet was generated by an ion source with a beam separator (Fig. 4). The grid system of the ion source has seven grid holes. One of them is made on the centerline, and the rest are arranged to surround the center one. Beamlets from the grid holes except the center hole are eliminated by the beam separator. The resulting ion-beamlet can simulate one of the beamlets generated by a multi-hole grid system and can be examined without being affected by other beamlets. A single-hole grid system would not simulate interference effects with other beamlets at their origins upstream of the screen grid.

Ion current profiles of this beamlet were measured by a Faraday probe array. The array consists of 32 probes arranged vertically, and is placed on an X-Y stage that moves along the beamlet axis and also perpendicular to it. Figure 5 shows examples of ion-current-density contours for the standard case. Measurements were conducted for various cases of the screen-to-accelerator grid separation and hole-center-to-center distance. Distortion factor is introduced to define a measure of how much the beamlet is distorted. Data were correlated in

terms of distortion factor and normalized perveance per hole.
 Results revealed that the distortion of the beamlet grows more serious in general as the normalized perveance per hole is decreased. However, hex-symmetrical distortion does not appear for the case that the hole-center-to-center distance is large enough.

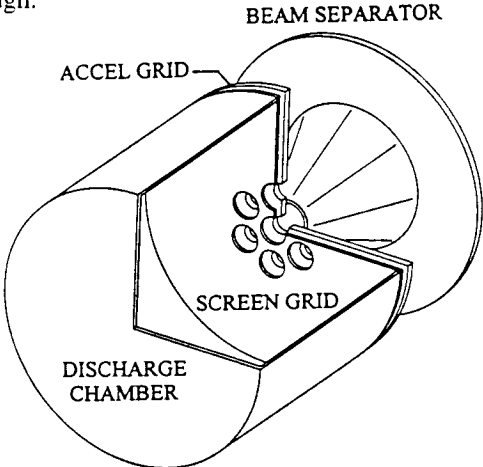


Fig. 4 Ion source with a beam separator for single beamlet generation.

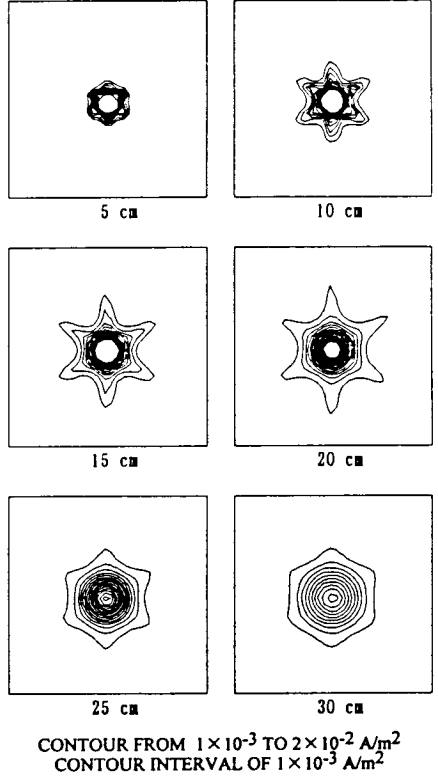


Fig. 5 Examples of ion-current-density contours. (Distance from the ion source is shown below each.)

Toshiba Corporation

Toshiba encourages 25mN class ion engine system for N/S station keeping of geosynchronous satellite and 150mN class ion engine system for orbit transfer vehicle in the electric propulsion field.

25mN ion engine Toshiba developed power processing units (PPU) and sequence controller (TCU) for ion engine subsystem of EST-VI which was launched in 1994.

As for COMETS, Toshiba is responsible for the ion

engine subsystem (IES) integration and manufacturing PPU/TCU. (Fig. 6) Toshiba carried out acceptance test of IES including ion thrusters, propellant management units, and valve drive electronics which were made by Mitsubishi Electric Corporation and certified that performance of IES satisfied its specifications. The design of COMETS IES is fundamentally the same as that of ETS-VI IES. (Fig. 7) Table 1 shows COMETS IES data.

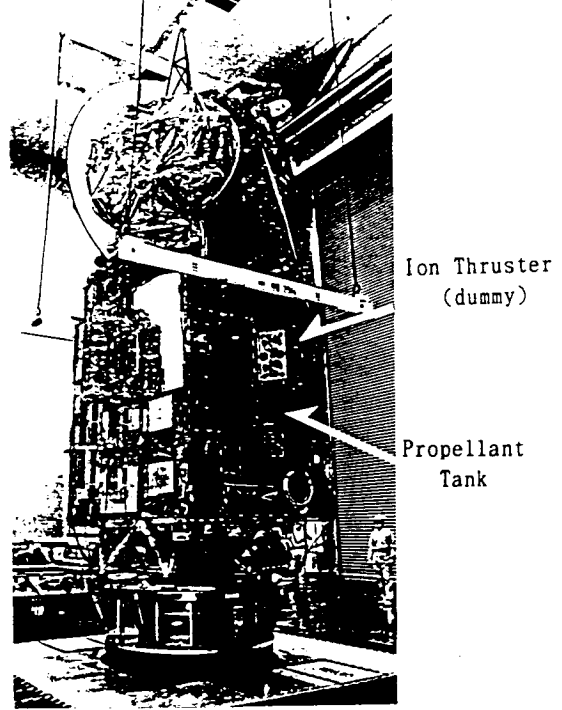


Fig. 6 COMETS

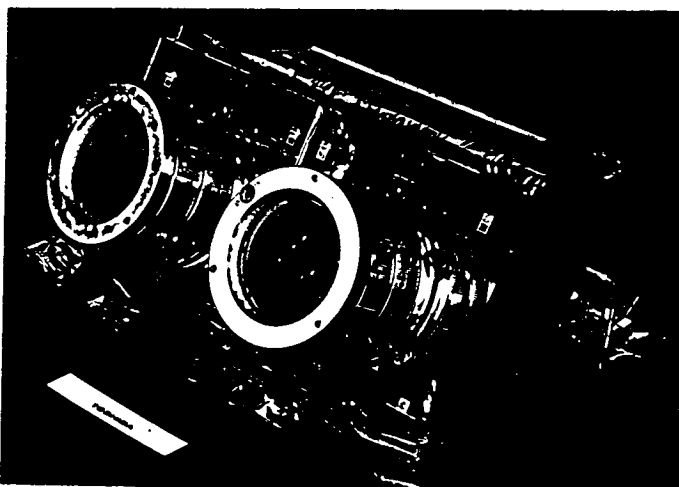


Fig. 7 Ion thruster (Flight model).

Table 1 COMETS IES DATA	
Thrust	: 23.3mN(thruster)
Specific Impulse	: over 2906sec(thruster)
Consumption Power	: 1633W
Dry Mass	: 98kg
Propellant Mass	: 16.5kg
Mission Duration	: 3years
Operating Time	: 2349hours
Operating Cycle	: 626cycles

150mN ion engine The activity on 150mN ion engine is mentioned in the section of NAL/NASDA/Toshiba of this paper.

NAL / NASDA / Toshiba Corporation

A 35-cm diameter ring-cusp xenon ion thruster for primary propulsion was designed, fabricated and tested to establish a lifetime design.⁵ It is the first breadboard model BBM-1 and was designed by modifying the second laboratory model LM-2.⁶ Major modifications of target performance are a startup time of 10 min and an operating time above 100 h. The BBM-1 thruster (Fig. 8) was designed to produce a thrust of 150 mN and a specific impulse of 3,500 s at the xenon flow rate of 3.27 A equivalent in the nominal operating condition. It has external dimensions of 45 cm in diameter and 29 cm in length and weighs 11.5 kg.

The BBM-1 thruster was operated stably for 100 hours at the beam voltage of 1 kV and the beam current of 2.9 A. Performance tests showed the ion production cost of 139 W/A under the following conditions; the propellant utilization efficiency of 90%, the discharge voltage of 28.8 V, the accelerator grid voltage of 300 V, the accelerator grid current of 13 mA to 16 mA, and the decelerator grid current of 6 mA to 12 mA. The performance reached the target except the startup time of about 20 min and the highest magnet temperature of about 218 °C.

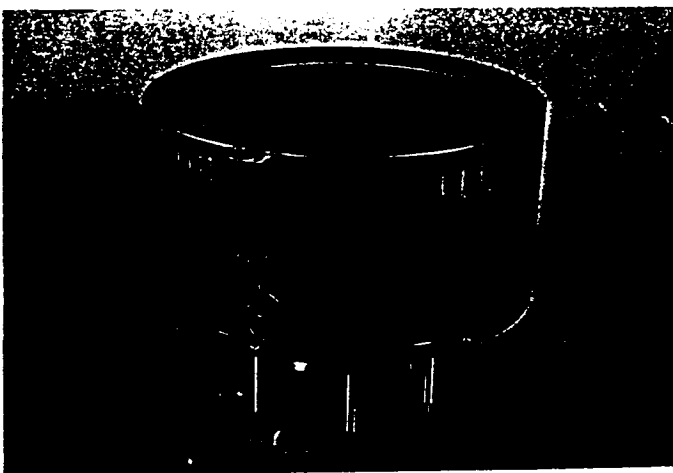


Fig. 8 NAL/ NASDA/ Toshiba 150 mN thruster BBM-1.

Mitsubishi Electric Corporation (MELCO)

Development of 25 mN ion engine subsystem (IES) for ETS-VI was completed. It was successfully operated on orbit, and the performance data were obtained.⁷⁻⁹ The specific impulse was about 3000 sec at 25 mN nominal operating point, and the total operating time (sum of four thrusters) was about 160 hours.

On IES for COMETS, the acceptance tests of each component and subsystem have been completed, and now, COMETS is standing by for launch in 1997.

For commercial use of ion engine, improvements of the same type of IES is now undergoing. The substances are as follows: 1) Life time of thruster is to be extended by improving ion production efficiency to decrease discharge voltage, by changing materials of grids to lower the sputter yield, and so on. The object is application to 2 ton class, 15 years life satellite. 2) The cost of the IES is to be reduced by reconsideration of subsystem construction, propellant

managing unit construction, and so on.

Breadboard model of 150 mN class ion thruster (XIES-150) has been fabricated under the contracts with NASDA and NAL. We put the thruster to the test and got the initial performance data. For the next step, we press for improvement in performance by changing the parameters for operation such as mass flow rates, the position of the magnets, and so on.

Ion optics made of carbon-carbon composite for 20 mN class ion thruster are fabricated under the contract with NAL. By improving the manufacturing process of the screen grid, almost all the carbon fibers are not cut off, and we expect the grid to be more rigidly than those currently in use.

Tokyo Metropolitan Institute of Technology

C₆₀ application to ion thruster¹⁰⁻¹³ C₆₀ application to the electron bombardment ion thruster where several considerations in its design were taken into accounts to prevent the C₆₀ re-solidification, fragmentation and multi-ionization was evaluated. Using this new designed thruster and crucible shown in Fig. 9, "Propellant Feed " and "Ionization and Beam Extraction " were examined. As a result, the sublimated C₆₀ flow rates of 0.89 SCCM, 2.38 SCCM and 4.89 SCCM (2.6 mg/s) against the power applied to the crucible heater; 26 W, 31 W and 36 W, were obtained, respectively. Moreover, as summarised in Table 2, the performance of this thruster (maximum thrust : 3.4 mN) was evaluated. In order to push forward this study, 1) the improvement of the effective plasma confinement and 2) more detailed experiments and evaluations for the optimization of the discharge voltage will be necessary.

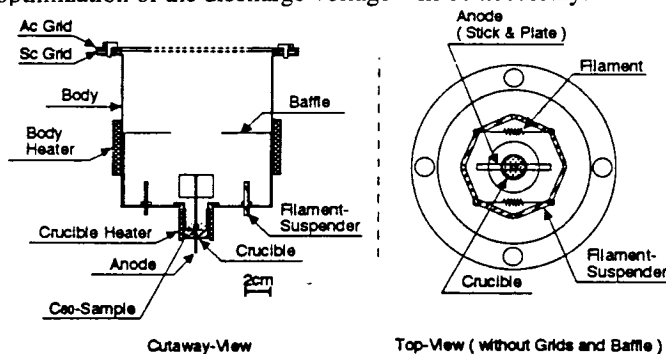


Fig. 9 C₆₀ ion thruster.

Table 2 Summary of C₆₀ ion thruster performance.

Effective Dis.-Voltage, Vd' , V	48.0
Filament Power, Pf , W	104
Discharge Power, Pd , W	70
BodyHeater Power, Phb , W	400
Cruc.Heater Power, Phc , W	36
Effective Flow Rate, \dot{m}' , SCCM	3.9
Net Accel. Voltage, Vsc , V	700
Target Current, I_t , mA	33.0
Accel Current, I_{ac} , mA	3.0
Extract Current, I_{ex} , mA	36.0
Thrust, mN	3.37
Propellant Util. Efficiency, %	12.2

Study on RF Ion Thruster¹⁴ In order to improve the RF ion thruster performance, considering the skin effects in the generated RF plasma column, the effects of the propellant feed method to the discharge chamber were evaluated by the diagnosis of the plasma properties using the double probe method. The results can be summarized as follows. The plasma properties in the discharge chamber depend on the feed method and by the reform of it as the electron temperature profile is flat, an RF power is transmitted effectively to the generated plasma, when the electron number density is increased. The more the electron number density adjacent to the grid is, the more the extraction ion beam is obtained.

MPD/arcjet thruster

Institute of Space and Astronautical Science (ISAS)

EPEX (Electric Propulsion Experiment) onboard SFU (Space flyer unit) An MPD (Magnetoplasmadynamic) arcjet is one of the electric propulsion principles based upon the electromagnetic acceleration of the plasma created by high current arc discharges and their self-induced magnetic field. Due to recent demands of relatively low power consumption ranging from several hundreds watts to 1 kilowatt in space, this MPD thruster system works in repetitively pulsed mode without any external magnetic fields applied.¹⁵ The discharge current was created by a capacitor bank that is so-called a Pulse Forming Network consisting of multi-staged LC-ladder network. The MPD thruster system was tested on the ground in 1988 as a full-scale model of 1 kW, however, the Space Flyer Unit (SFU) resource limitation has reduced the number of LC-ladder network down to only single stage so as to minimize the experiment weight. Due to this decision the EPEX (Electric Propulsion Experiment) has been regarded as a function verification test of the MPD arcjet system in space.

The EPEX objectives are as follows: 1) Checkout the system integrity after launch and space environment, 2) Verification of propulsive function, and 3) Dump residual hydrazine safely into space. The last objective was the most important one from the view point of SFU safety compliance to the Space Shuttle retrieval. The EPEX was recommended to use liquid hydrazine as the propellant, targeting a future application sharing the propellant with conventional hydrazine gas jets. A great deal of efforts were paid to the prevention of hydrazine freezing during the SFU flight and the complete dump of the residual hydrazine. Only 130 g of hydrazine was allowed to load the EPEX propellant tank for the safety reason. The experimental period allocated to the EPEX was about 3 days on-orbit, however, the EPEX breadboard model successfully finished 600 hours consecutive firings (3 million shots) in 1988 and its endurance was already confirmed on the ground test. The SFU was launched on March 18, 1995 by the H-II TF#3 from Tanegashima Space Center and separated at 330 km. As the mission altitude was 486 km circular orbit, the SFU climbed up by her own gas jet thruster. After about 6 months experimental period that enabled 13 kinds of different experiments including EPEX, and after about 4 months bus checkout period, the SFU was grappled by a US Space Shuttle "Endeavour" on January 13, 1996 and successfully landed at Kennedy Space Center on January 20, 1996.

EPEX system definition The EPEX comprises a Thruster Head with 2 Fast Acting Valves (FAV), a 2,240 mF capacitor

bank (CAP) with a 2 mH inductance (CL), Charge Control Unit (CCU), Control & Monitor Unit (CMU), FAV & Trigger Driver Unit (FTDU), Valve & Relay Driver Unit (VRDU), Terminal Unit (TRU), and Propellant Supply System¹⁶. Besides these exclusive components and subsystems, Dedicated Experiment Processor (DEP) is installed on the SFU Payload Unit (PLU-2). The PLU-2 accommodates electronic devices for 3 different kind of experiments, EPEX, two-dimensional deploying array (2D), and high voltage solar array (HV) experiment (Fig. 10). The DEP installs each of the experimental software and interfaces with the SFU bus for transmitting bus commands and packeting the telemetry data to and from CMU and other experimental processor. The EPEX system weight amounts to 40.235 kg excluding the DEP but including propellant (Fig. 11).

All the electrical power was supplied from the SFU bus line at DC 32.5 - 50 volts and the maximum available power for the EPEX was 430 W during the sunshine period. During the sunshade period, it was 225 W. To keep the hydrazine temperature away from freezing at 2 °C and to keep the electronic devices temperature properly, the EPEX has 80 W heaters totally in the PLU-2.

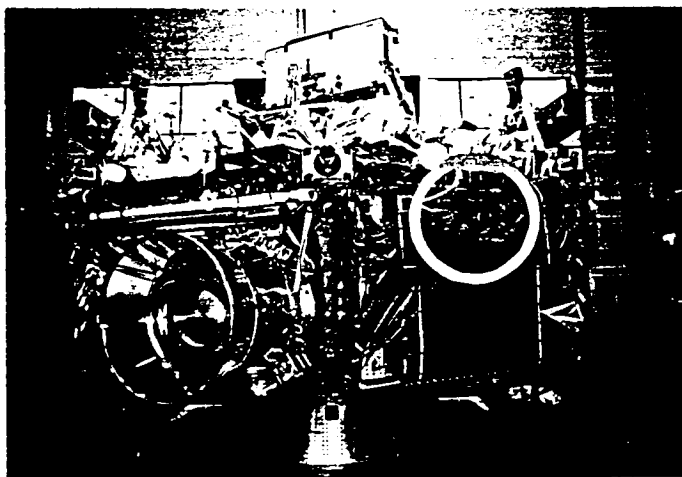


Fig. 10 EPEX system installed on the SFU. (Circled : MPD arcjet thruster)

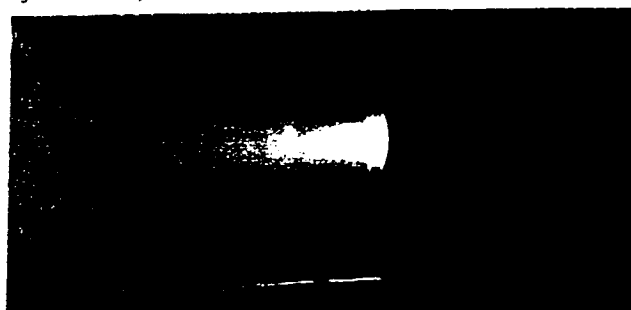


Fig. 11 MPD thruster firing test on the ground.

EPEX results After the SFU injection into a mission orbit, the minimum success was defined to checkout the EPEX electrical system. All the heaters were verified to function properly to maintain the PLU-2 temperatures and the DEP was powered on during the SFU orbit raising. The first experimental checkout was to verify charging up capability of the CCU and PFN as well as the control capability of the CMU. These were successfully conducted and also the capacitor dump capability through the resistive load was

demonstrated.

Since the charging capability was guaranteed, the next verification is the capability of propellant feed system. There were no signs of propellant or pressurant leakage. The firing sequence was started with the propellant valve open and it was confirmed that the gas generator worked properly and the secondary tank was filled with the hydrazine decomposed gas up to about 7 kgf/cm². This value was originally set as 10 kgf/cm², however, the reduction of propellant loading required less propellant consumption on-orbit. The Shot-by-Shot firing test was automatically controlled by a bunch of commands sequence Functional Objective (FO) stored in the DEP and successfully processed by the CMU.

The propulsive function of the MPD arcjet thruster system was tested by a consecutive firings during 37 minutes for sunshade period or 45 minutes for sunshine period at a repetition rate of 0.5 Hz and 1 Hz, respectively. This was also successfully controlled by FOs automatically and autonomously. There were no sign of firing sequence interruption and the propellant supply was successfully maintained by the feed-back loop control of the propellant valve that should open periodically as function of the secondary tank reservoir pressure. The threshold pressure was 5.9 kgf/cm² and this is sufficiently sensitive to keep the propellant mass shot constant.

The EPEX thrust vector was designed intentionally to deviate from the center of gravity of the SFU by about 25 cm torque arm. This deviation acts on the SFU attitude control system as the disturbance comparable to the largest natural disturbance of the gravity gradient. The EPEX torque vector is opposite to the gravity gradient and it was evaluated from the quantity of the momentum wheel control that should cancel the EPEX oriented disturbance. On the other hand from the telemetry data, the propellant mass shot was evaluated from the pressure decay of secondary tank reservoir and the number of firings during that decay. This is so-called a blow-down method. After manipulating these quantities, the EPEX showed the specific impulse of 1,111 sec and the thrust-to-power ratio of 20 mN/kW as the top values during the main arc discharge. These values should be expected if the full-scale 1 kW PFN was installed onboard the SFU.

For the rest of time allocated to the EPEX, similar consecutive firings were conducted as many times as possible. These were run with different firing repetition rates such as 0.5, 1, 1.4, and 1.8 Hz (Fig. 12).

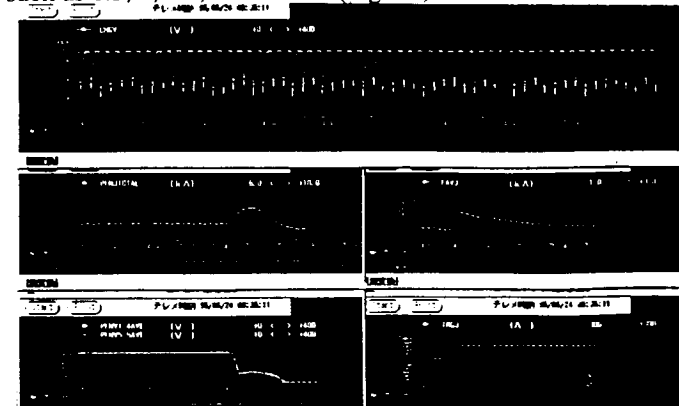


Fig. 12 Typical telemetry data of EPEX firing : Charge & Discharge voltage of the PFN, discharge current waveform, discharge voltage waveform, FAV driving current and trigger level status.

All the experiments were successfully tested and the accumulated firing number of EPEX on-orbit amounted to over 40,000 shots. The averaged misfiring rate resulted in less than 0.3%. This rate is very low in the low repetition rates but at 1.8 Hz it had an increasing tendency.

After the EPEX completion, the residual hydrazine was successfully dumped into space together with the nitrogen pressurant by opening 3 latching valves. It took about two minutes to evacuate the propellant tank and it took about 2 weeks to dry out the internal surface of the tank and lines. The 3 latching valves were kept open for about 1 month to ensure the hydrazine evaporation. By closing these latching valves on August 23, 1996 the EPEX completed all the planned experiments onboard SFU (Fig. 13).

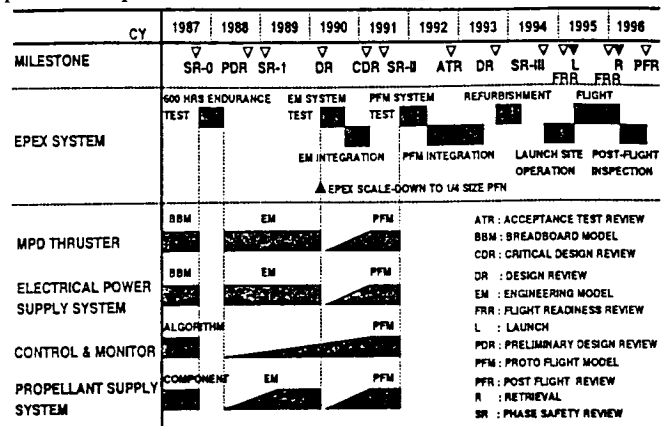


Fig. 13 Development history of EPEX.

DC arcjet research A 300 W class low power DC arcjet SAGAMI-III has been studied in ISAS for these 5 years by using N₂+2H₂ gas mixture.¹⁷ This study was originated from the requirement of realistic power consumption in the scientific satellites or other relatively small-scale satellites. The SAGAMI-III arcjet thruster was designed to be small-sized with small diameter constrictors ranging from 0.3 to 0.5 mm. This implies essentially a high pressure operation of plenum chamber up to several kgf/cm² and it has brought us a crucial problem of propellant permeation through the interelectrode insulator. The SAGAMI-III improved the interelectrode insulator material from conventional boron nitride to low-porosity ceramic one to demonstrate thrust efficiency as high as 37 % at an Isp of 440 sec with 350W input power (Fig. 14) and to have confirmed more than 1,000 cycle start-up capability without any significant damages.¹⁸⁾ On the other hand the physical background of stable operation under such low power is now investigated using a 2-dimensional DC arcjet that enables the flow visualization of SAGAMI-III class small arcjets. The discharge mode transition from low- to high-voltage has been examined to pursue the low power limit of DC arcjet thruster (Fig. 15).

MPD arcjet research A 2-dimensional MPD arcjet has been studied for many years in ISAS to clarify the flowfield correlation with the thrust performances. Recently one of the most significant performance improvement was found experimentally by the employment of a short cathode with a convergent-divergent anode nozzle (Fig. 16). Apparently the flowfield was dominated by the magnetosonic condition that should occur at the throat in such configuration, and it can shift upstream when a simple divergent nozzle is employed. The simple divergent anode-nozzle has been regarded as the

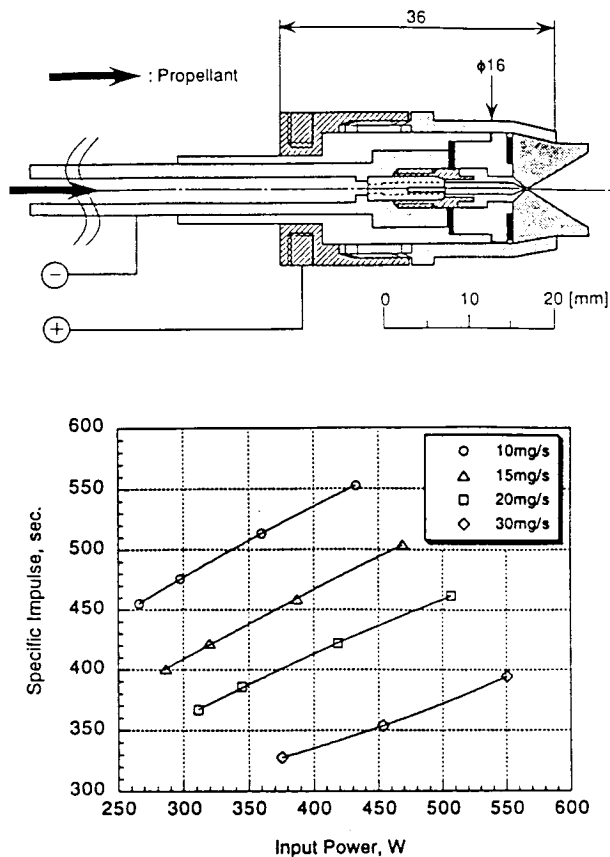


Fig. 14 SAGAMI-III 300-W class DC arcjet thruster and its thrust performance.

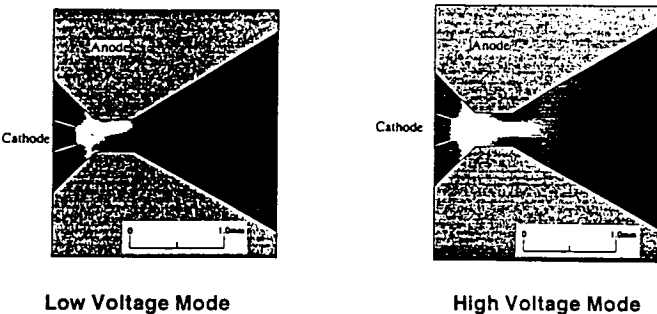


Fig. 15 Flow visualization of sub-millimeter arcjet constrictor.

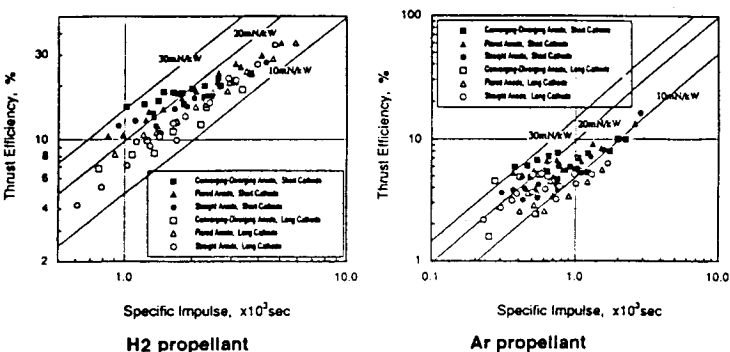


Fig. 16 2-dimensional MPD arcjet experiments using various electrode configurations.

best shape for the MPD arcjet in the Isp range of 1,000 to 2,000 sec, however, the 2-dimensional numerical analysis predicted occurrence of super-magnetosonic heating of plasma at the short-cathode tip region (Fig. 17) and that resulted in low thrust performance. Therefore the preliminary conclusion for the best performance is strongly related to the position control of magnetosonic velocity so as to avoid super-magnetosonic heating.¹⁹

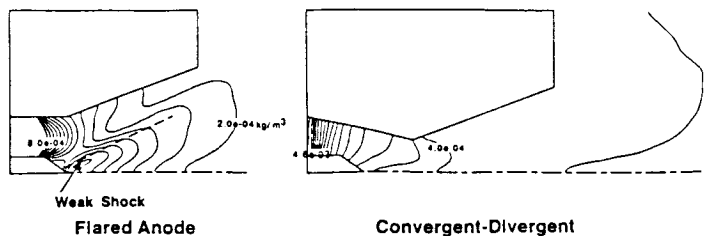


Fig. 17 Numerical simulation of super-magnetosonic MPD flow (Density distribution).

Ishikawajima-Hirata Heavy Industries Co., Ltd. (IHI)

IHI has now a proud of contributing in the success of EPEX mission. In the development of 1 kW-class MPD arcjet system for the EPEX mission, (Fig. 18) IHI had roles of developing a high performance MPD thruster, a propellant supply system and a thermal control system for propellant (hydrazine) and electronic equipment and supporting the EPEX operation from launch to the end of mission on orbit. The figure IHI-1 shows the MPD thruster, which composes of a cathode electrode made from barium-oxide impregnated porous tungsten, a segmented anode electrode from molybdenum and 2 sets of Fast Acting Gas Valve. The telemetry data showed the MPD thruster system had a good interface with SFU bus system and produced almost same thrust performance as ground test results. The appearance checkout after retrieval showed no abnormal on the surface and in the discharge chamber of MPD thruster. Detail performance checkout will be conducted and will confirm an establishment of design technology for 1 kW-class MPD thruster system.

IHI is focusing on developing a low power (1 kW and less) DC arcjet thruster system. The low power and small thruster system seems to be attractive and promising for altitude control of satellite of 1 ton and less. Feasibility study has been finished. The system has achieved specific impulse higher than 500 s and efficiency of power control unit higher than 90 %. Propellant flow control technology has been also established. Flight model of thruster module is being developed now.

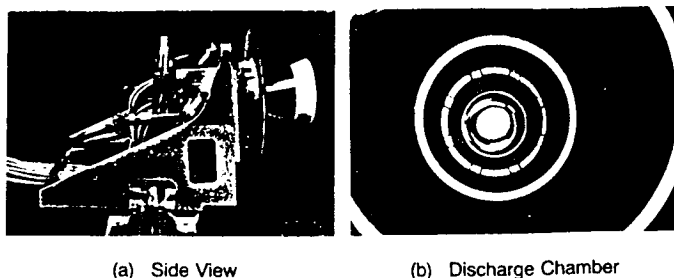


Fig. 18 MPD thruster module loaded on SFU-1

Osaka university

Quasi-steady MPD arcjet research Plasma diagnostic measurement and flowfield analysis in quasi-steady MPD channels with electrodes 200-300 mm long, almost realizing only electromagnetic blowing acceleration, i.e., one-dimensional flowfield, were made.^{20,21} The measured current fractions on the electrodes intensively increased near the downstream end of the channel regardless of gas species. Current slightly concentrated near the inlet with Ar at high magnetic Reynolds numbers. The experimental results agreed roughly with analyzed ones. Accordingly, the axial variations of Lorentz forces inferred from the measured physical properties and the calculated plasma velocities, as shown in Fig. 19, showed that there were two acceleration zones near the inlet and the outlet with Ar at high magnetic Reynolds numbers, although plasma was expected to be accelerated only near the outlet with Ar at low magnetic Reynolds numbers and with molecular gases. Also, the influence of applied magnetic fields on thruster performance and energy balance was studied using an MPD arcjet periodical operation system.

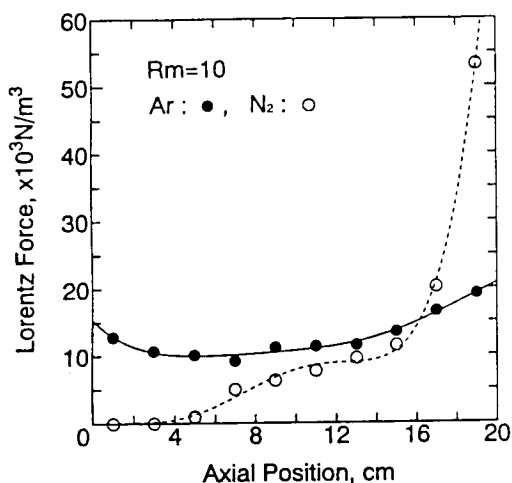


Fig. 19 Axial variations of Lorentz forces inferred from measured current fractions on MPD channel electrodes for Ar and N₂ at magnetic Reynolds number of 10.

Steady-state arcjet thruster research & development

The laboratory-model radiation-cooled arcjet thruster RAT-VII, as shown in Fig. 20, was operated in the electric power range of 300-1100 W with a mixture of nitrogen and hydrogen simulating hydrazine at mass flow rates of 15-25 mg/s although the arcjet geometry had already been designed optimally for 1 kW class operation.²² In order to achieve high-performance stable operations around 500 W, the electrode gap was shortened from 0.2 to 0.1 mm, and the constrictor diameter was decreased from 0.5 to 0.4 mm. Furthermore, the effect of propellant swirl flow injection into the arc chamber was examined. As a result, the arcjet with an electrode gap of 0.1 mm and with swirl flow injection stably operated below 500 W, and a high performance of thrust efficiency 42 % and specific impulse 458 sec was achieved at 500 W.

Spectroscopic measurement and numerical analysis were conducted to understand the flowfield in a 10 kW class arcjet thruster.^{23,24} Nitrogen and ammonia were used as propellants. In the expansion nozzle, the pressure and the electron density

drastically decreased downstream, and therefore the plasma was in thermodynamical non-equilibrium although the plasma in the constrictor was expected to be nearly in a temperature-equilibrium condition. The radial profiles of the physical properties, as shown in Fig. 21, showed that there existed a core flow with high vibrational and rotational temperatures and large electron number densities on the center axis even at the nozzle exit. The calculated energy deposition showed that the frozen flow losses were mainly occupied by energies of dissociation, ionization and translational motion.

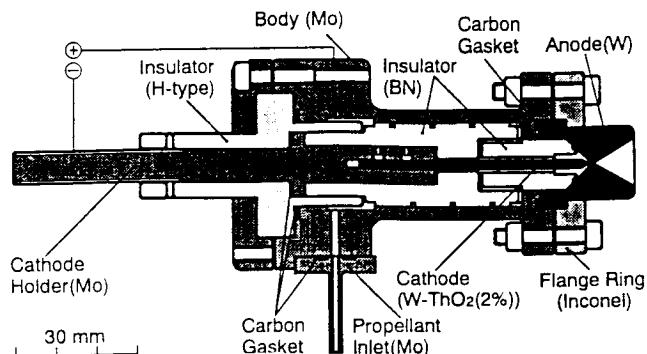


Fig. 20 Cross section of radiation-cooled arcjet thruster RAT-VII.

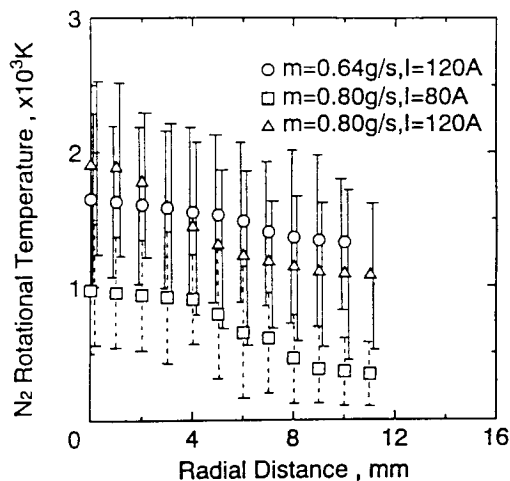


Fig. 21 Radial profiles of N₂ rotational temperature at expansion nozzle exit for nitrogen propellant.

Non-propulsion applications For applications of quasi-steady MPD arcjets to ceramic coatings, an MPD arcjet with a cathode covered with a ceramic material was developed.²⁵ The front velocities of ablated ceramic Al atoms inferred with a streak camera were much higher than velocities of 200-500 m/s for conventional plasma torches. This is effective for deposition of rigid films adhering strongly to substrate surfaces. The MPD plasma spraying showed that a dense uniform ceramic film with above 1,200 Vickers hardness was deposited.

The influence of high-energy charged-particle bombardment and UV light irradiation on chemical structure of polyimide films was investigated to clarify the mechanism of material degradation in space.²⁶ The films were exposed to oxygen or nitrogen ion beams with 0.5-1 keV, to electron beams with 20-30 keV and to UV and visible light of 250-600

nm. X-ray photoelectron spectroscopic analysis showed structural changes of the exposed polymers. The optical properties of transmittance and reflectance were also found to be degraded by the complex exposure.

A ground facility was developed to simulate the interaction between materials and space plasma in LEO.²⁷ The space plasma simulator consisted of a vacuum tank 0.7 m in diameter and 1.5 m long, two turbo-molecular pumps with pumping speeds 5 and 3 m³/s, respectively, achieving some 10⁻⁴ Pa, and an electron cyclotron resonance plasma source of a magnetic-expansion-type plasma accelerator. Plasma properties of plasma density, electron temperature, ion velocity and atomic oxygen flux were measured. Furthermore, plasma emission spectroscopic measurements and preliminary tests of exposure of polymers to plasma flows were conducted. The simulator was found to have a high potential for ground tests.

Kyushu university

Since eight years, computational studies of a flow in a radiation-cooled arcjet thruster with 1kw power have been conducted.^{28,29} Argon has been used as propellant gas and the computations have been done for the same geometry of an arcjet thruster as used in laboratory experiments. The propellant gas is heated to a high temperature by Joule heating, ionized partially and then accelerated through a nozzle. This process is expressed by flow equations coupled with the equations for electron mass conservation, Ohm's law and continuity of electric current. Navier-Stokes equations were employed for flow equations and an equilibrium radiation condition that heat flux from gas to wall is equal to heat release from wall by radiation is put on the walls to express radiation cooled wall. Moreover, in this study nonequilibrium ionization-recombination was considered. Temperature contours computed for mass flow rate of 0.1g/s and arc power of 1kw are shown in Fig. 22. Computed thrust and specific impulse were compared with the experimental ones and satisfactory agreements were obtained.

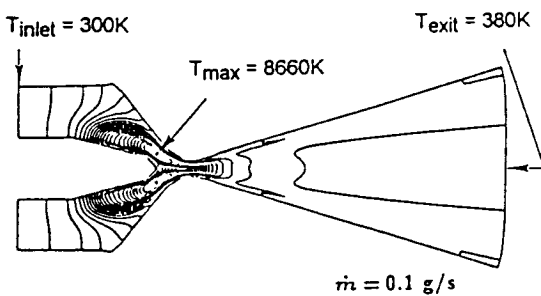


Fig. 22 Temperature contours.

A comparison of computed and experimental thrusts is shown in Fig. 23. At present, the computations developed for argon is being extended to an arcjet thruster with nitrogen as propellant. Temperatures of internal energy modes are separately treated here, that is to say, a three temperature model composed of heavy particle translational temperature, vibrational temperature and electron translational temperature is employed while translational temperature is assumed to be equal to rotational temperature. Numerical calculations generally need very long computing time, so that nothing

would be better than quasi one-dimensional calculation, if that could give satisfactory results to an industrial thruster design. On the view of this point, quasi one-dimensional calculations which are available as simple design tool were attempted and the results were compared with previous experiments.³⁰ In this analysis,³¹ discharge power is put into propellant gas as heat input then total enthalpy of the propellant gas is increased. However, it is considered that the discharge power is employed not only for elevation of the propellant gas temperature but also for ionization.

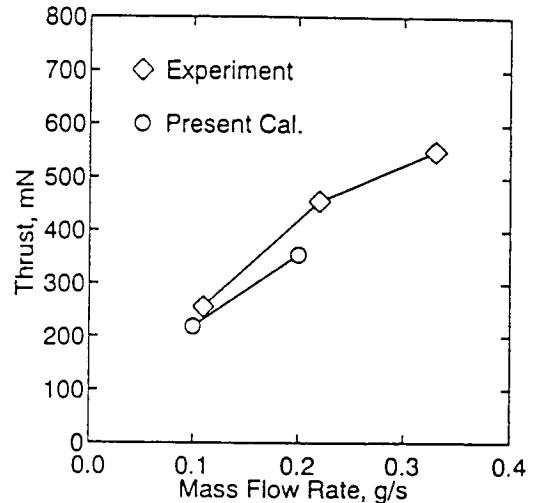


Fig. 23 A comparison of calculated and experimental thrusts.

Tohoku university

In the Department of Electrical Engineering of the Tohoku University, a quasi-steady MPD arcjet is used for producing a high-density-plasma flow to develop new diagnostics and to study magnetohydrodynamic phenomena such as a nonlinear Alfvén wave and field-line reconnection. The MPD arcjet is installed in the HITOP device, which is a large cylindrical vacuum chamber (diameter $D = 80$ cm, length $L = 320$ cm) provided with external magnetic coils. The MPD arcjet can be operated with/without the externally applied magnetic field. The plasma flow characteristics are currently being measured by several diagnostics. An arc current up to 10kA with a typical arc voltage of 200V is fired through a pulse forming circuit, and a high density arc plasma is blowing out quasi-steadily during 1 ms.

A high density (more than 10^{16} cm⁻³) plasma is formed in the muzzle region of the MPD arcjet, the inner diameter of which is 3 cm. The plasma is accelerated in the axial (Z -axis) direction by the $J \times B$ force, and expands in the large vacuum tank. Radial profile of the plasma density and electron temperature is measured by Langmuir probes. In the expanded plasma with a half-maximum diameter of 20 cm, on-axis electron density and temperature are 7×10^{13} cm⁻³ and 5 eV, respectively. The plasma flow is characterized by a Mach number M which is defined as the ratio of the plasma flow velocity to the ion acoustic velocity. The Mach number is measured by a Mach probe and is typically 2. The ion temperature and flow velocity can be measured by a time-of-flight (TOF) neutral particle energy analyzer. A TOF analyzer

is recently set at the end of the vacuum chamber to detect charge-exchanged neutral particles as a function of the particle velocity V_z . A spectrometer is also being installed to measure ion temperature and flow velocity.

At Institute of Fluid Science, also Tohoku University, analytical work on electromagnetic accelerations is conducted. Self-field acceleration, swirl acceleration, Hall acceleration and electrothermal acceleration are combined together to yield a simple formulation.³²

Hall thruster

University of Tokyo

In a Hall thruster, the assumption of quasi-neutrality cannot be used in the neighborhood of the anode and of the wall surface owing to the existence of the sheath. In addition, charge neutrality can be violated also in a low-density plasma with the strong magnetic field such as that in the downstream region of the acceleration channel. Therefore, we have developed the particle simulation method to examine plasma phenomena in these regions.³³ In our code, electron and ion trajectories are followed in time by the particle-in-cell (PIC) method coupled with the Monte Carlo technique which presumes the electrostatic approximation. Simulation results show that the plasma properties can fluctuate in the azimuthal direction. Figure 24 is the contour of the space potential in r - θ plane, indicating that it periodically changes with the azimuthal angle. It changes also with time, of which frequency is much smaller than the plasma frequency. With the resulting fluctuant azimuthal electric field, electrons come to more easily run across the magnetic field lines. Typical distributions of the plasma density and the space potential in the acceleration channel are shown in Fig. 25, and qualitatively agree with the measured distributions. These results suggest that this method is useful to examine plasma flow in a Hall thruster.

At University of Tokyo, 1kW-class Hall thruster has been developed and tested to examine its thruster performance characteristics and acceleration processes. The schematic of the thruster is shown in Fig. 26. A hollow cathode is installed on thruster axis. From thrust measurement, thrust efficiency increases with increasing discharge voltage and more than 40% thrust efficiency has been obtained at discharge voltage 300 V.



Fig. 24 Contour of the space potential in the acceleration channel.

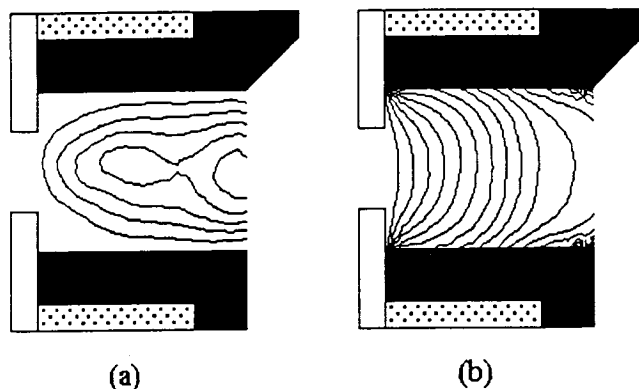


Fig. 25 Distributions of plasma properties in the acceleration channel. (a) Plasma density, (b) Space potential.

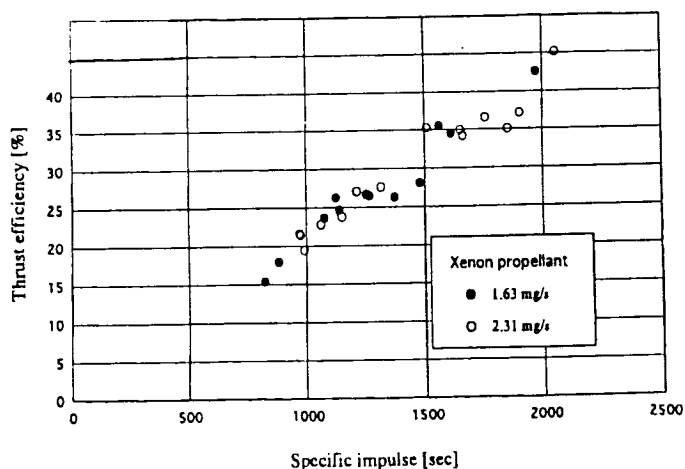
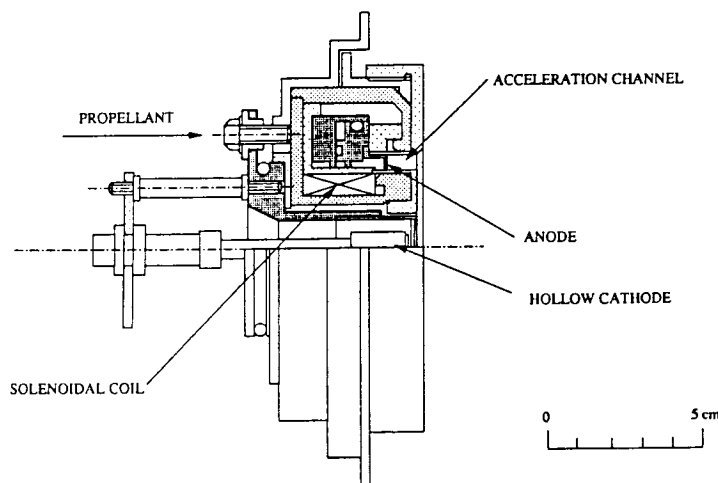


Fig. 26 1 kW-class Hall thruster and the thrust efficiency

Nagoya university

A variable channel Hall thruster has been experimentally tested for the research of the acceleration hannel optimization.³⁴ (Fig. 27) Channel length is variable from 1.5 mm to 10 mm. The total beam-current was measured using a multi-ion-collector system. To precisely estimate the acceleration efficiency, the current decrease due to the charge exchange collision in a vacuum chamber is compensated by

exponential curve-fitting.³⁵ The maximum ion-current was extracted from the channel at the length, $L = 4$ mm for argon propellant. The optimum channel length was mostly independent of the operational condition, such as the discharge voltage and the magnetic induction.

Using a simple plasma discharge model, the optimum channel length is theoretically investigated. In this model, the ion-production coefficient and the ion-loss fraction are expressed as a function of the channel length. Taking a derivative of the acceleration efficiency, optimum channel length can be expressed by a algebraic equation. The theoretical optimum length is a function of the channel width and the neutral mean free-path for ionization collisions as shown in Fig. 28. When the mean free-path is less than 1 mm, the optimum channel length is almost same as the neutral mean free-path, and it approaches to the channel width with the increase in the mean free-path.³⁶

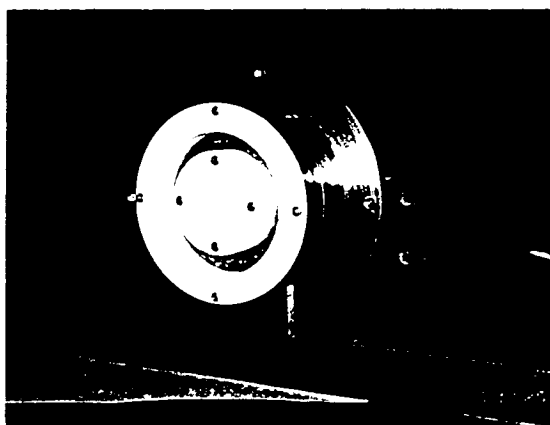


Fig. 27 A variable-channel Hall thruster.

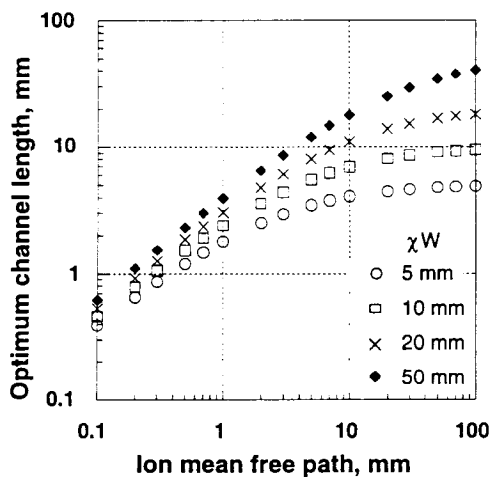


Fig. 28 Theoretical optimum-channel-length.

Mission analysis

As recent interest in electric propulsion has been focusing on mission applications, mission analysis and optimization of the electric propulsion system is becoming more important in order to fully utilize electric propulsion performance and to help design electric thruster more appropriate for use.

Recent advance in optimization provides efficient and robust algorithms, such as Sequential Conjugate-Gradient Restoration Algorithm (SCGRA) and Direct Collocation with

Nonlinear Programming (DCNLP). The researchers of University of Tokyo have been using the SCGRA and DCNLP for solving low-thrust trajectory optimization problems and found each method has both merits and demerits in using electric propulsion mission analysis. The SCGRA is low in computation cost, however, tends to lose convergence when an initial estimate is poorly given. The DCNLP is robust even against a poor initial estimate, however, requires huge computation memory and time. Therefore, an efficient interplanetary trajectory optimization code has been developed for electric propulsion system study by combining the above two numerical optimization techniques.³⁷ In the combined method, the DCNLP is used to calculate a rough estimate and the SCGRA then follows it to obtain a final estimate with reasonable accuracy.

Typical computation time for solving interplanetary trajectory optimization problem is plotted in Fig. 29 as a function of number of time steps. Computation time was measured on the personal computer (~100MIPS) until the solution converged to a specified tolerance. Computation time in the DCNLP significantly increases with number of time steps while it slightly increases with number of time steps in the combined method. (It should be noted that the convergency of a solution is guaranteed in the DCNLP and combined method and not in the SCGRA. In this calculation, the SCGRA code did not yield a convergent solution, therefore, the SCGRA's computation time was omitted in Fig. 29.) Therefore, the combined method saved computation time without spoiling robust convergence. shown in Fig. 30 is an example of optimized trajectories for Asteroid mission.

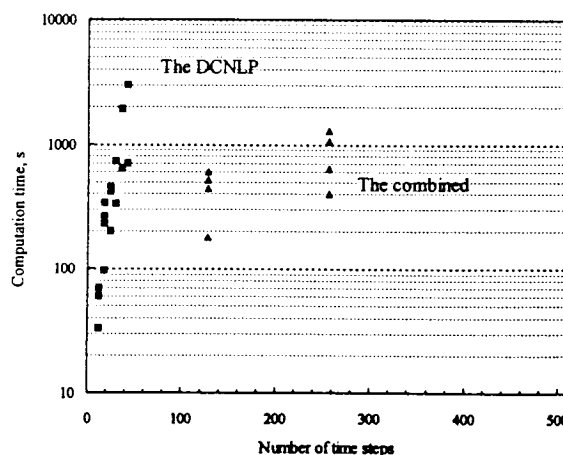


Fig. 29 Typical computation time.

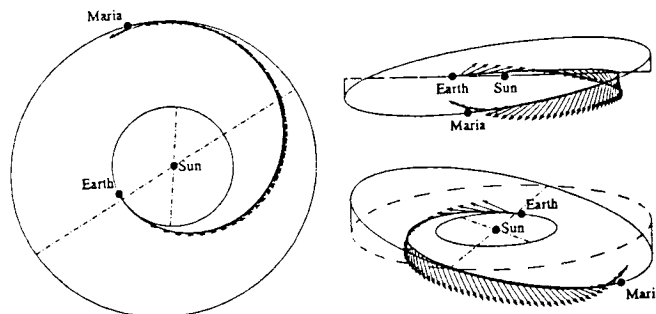


Fig. 30 Optimal trajectories for asteroid mission.

Acknowledgement

The work described in this paper was carried out by the members of the national space development agency of Japan, the national aerospace laboratory, the institute of space and astronautical science, Mitsubishi electric corporation, Toshiba corporation, Ishikawajima-Harima heavy industries, Tokyo Metropolitan Institute of Technology, Osaka university, Kyushu university, Tohoku university, the university of Tokyo. The author gratefully acknowledges the contributions of these members.

References

- ¹ Miyazaki, K., Hayakawa, Y., Kitamura, S., "Direct Thrust Measurement of a 14-cm Xenon Ion Thruster," Int'l Symp. Space Tech. and Sci., ISTS-95-a-3-24p, 1996.
- ² Hayakawa, Y., Miyazaki, K., Kitamura, S., "Performance Test of a 14-cm Xenon Ion Thruster," AIAA-92-3147, 1992.
- ³ Hayakawa, Y., Miyazaki, K., Kitamura, S., "Ion Beam Characteristics of a 14-cm Xenon Ion Thruster," AIAA-94-2852, 1994.
- ⁴ Hayakawa, Y., Kitamura, S., Miyazaki, K., "Beamlet Profiles from Multiple-Hole Ion-Extraction Systems," AIAA-96-3199, 1996.
- ⁵ Yoshida, H., et al., "Performance Characteristics of a 35-cm Diameter Xenon Ion Thruster," AIAA-96-2714, 1996.
- ⁶ Kitamura, S., et al., "Performance Characteristics of a 30 cm Diameter Xenon Ion Thruster," AIAA-94-2850, 1994.
- ⁷ Shimada, S., Nagano, H., et al., "Development of Ion Engine System for ETS-VI," IEPC-93-009, 1993.
- ⁸ Nagano, H., Gotoh, Y., et al., "On-Orbit Performance of ETS-VI Ion Engine Subsystem," IEPC-95-139, 1995.
- ⁹ Nagano, H., Gotoh, Y., et al., "Development and On-Orbit Operation of ETS-VI Ion Engine Subsystem," ISTS-96-a-3-18, 1996.
- ¹⁰ Nakayama, Y., Endo, N., Takegahara, H., "Study on C60 Application to Ion Thruster - Evaluation of Ion Production," AIAA-96-3210, 1996
- ¹¹ Nakayama, Y., Takegahara, H., "Study on C60 Application to Ion Thruster - C60 Feed and Ion Production," ISTS-96-a-3-08, 1996
- ¹² Nakayama, Y., Takegahara, H., "Fundamental Experiments of C60 Application to Ion Thruster," IEPC-95-88, 1995
- ¹³ Takegahara, H., Nakayama, Y., "C60 Feasibility Study on Application to Ion Thruster - Preliminary Experiments Using Electron Bombardment Thruster," AIAA-95-2665, 1995
- ¹⁴ Takegahara, H., Iwata, T., Nakamichi, T., "Study on the Performance Improvement of RF Ion Thruster - The Effects of the Propellant Feed System on the Plasma Properties," ISTS-96-a-3-25P, 1996
- ¹⁵ Toki, K., Shimizu, Y., Kuriki, K., Kuninaka, H., "An MPD Arcjet Thruster System for Electric Propulsion Experiment (EPEX) in Space," AIAA-94-2989, 1994.
- ¹⁶ Toki, K., Shimizu, Y., Kuriki, K., "An MPD Arcjet Thruster System Test Onboard SFU," ISTS-96-1-3-13, 1996.
- ¹⁷ Ogiwara, K., Hosoda, S., Suzuki, T., Toki, K., Kuriki, K., Matsuo, S., Nanri H., Nagano, H., "Development and Testing of a 300 W-class Arcjet," IEPC-95-017, 1995.
- ¹⁸ Ogiwara, K., Hosoda, S., Kimura, I., Matsuo, S., Nagano, H., Nanri, H., Toki, K., Kuriki, K., "Study of 300-W Class Direct Current Arcjet Thruster," ISTS-96-a-3-01, 1996.
- ¹⁹ Funaki, I., "Magnetohydrodynamic Flow in the MPD Arcjet," Doctor Thesis, University of Tokyo, 1995, in Japanese.

- ²⁰ Tahara, H., Mitsuo, K., Zhang, L., Kagaya, Y., Yoshikawa, T., "Plasma Features in Quasisteady MPD Channels," IEPC-95-116, 1995.
- ²¹ Mitsuo, K., Tahara, H., Andoh, Y., Kagaya, Y., Yoshikawa, T., "Arc Structure in a Quasi-Steady MPD Channel," ISTS-96-a-3-17, 1996.
- ²² Izumisawa, H., Yukutake, T., Andoh, Y., Onoe, K., Tahara, H., Yoshikawa, T., Ueno F., Ishii, M., "Operational Condition and Thrust Performance of a Low Power Arcjet Thruster," ISTS-96-a-3-23p, 1996.
- ²³ Tahara, H., Komiko, K., Zhang, L., Onoe K., Yoshikawa, T., "Plasma Features in a Medium-Power Arcjet," IEPC-95-16, 1995.
- ²⁴ Yonezawa, T., Tahara, H., Andoh, Y., Onoe, K., Yoshikawa, T., "Spectroscopic Measurement and Numerical Analysis of Thermal Non-Equilibrium Flow in a 10kW-Class Arcjet Thruster," ISTS-96-a-3-05, 1996.
- ²⁵ Tahara, H., Mitsuo, K., Zhang, L., Yasui, T., Kagaya, Y., Yoshikawa, T., "Ceramic Coatings Using Quasisteady MPD Arcjets," IEPC-95-178, 1995.
- ²⁶ Tahara, H., Zhang, L., Hiramatsu, M., Yasui, T., Yoshikawa, T., Setsuhara, Y., Miyake, S., "Exposure of Space Material Insulators to Energetic Ions," *J. Appl. Phys.*, Vol. 78, No. 6, 1995, pp.3719-3723.
- ²⁷ Tahara, H., Ogo, A., Zhang, L., Yasui, T., Yoshikawa, T., "Development of a Space Plasma Simulator Using an Electron Cyclotron Resonance Plasma Source and Its Applications to Material and Plasma Interaction Research," ISTS-96-b-38p, 1996.
- ²⁸ Okamoto, H., Nishida, M., Tanaka, K., "Numerical Studies of the Flow Fields in a Low Power DC Arcjet Thruster Using Navier-Stokes Equations," IEPC 91-113, 1991.
- ²⁹ Okamoto, H., Nishida, M., Tanaka, K., Beylich, A., "Numerical Simulation of the Performance of a Radiation-cooled 1kw DC Arcjet Thruster," IEPC-93-181, 1993.
- ³⁰ Tanaka, K., Tsuchiya, K., Kaita, K., Nishida, M., "Experimental Investigation on the Characteristics of a Low Power DC Arcjet Thruster," IEPC-88-109, 1988.
- ³¹ Nishida, M., Okamoto, H., "Simple Estimation of the Performance of a Low Power Arcjet Thruster," IEPC-95-22, 1995.
- ³² Sasoh, A., "Simple Formulation of Magnetoplasmadynamic Acceleration," *Physics of Plasma*, Vol. 1, No. 3, pp. 464-469.
- ³³ Hiraoka, M., "Numerical Simulation of Plasma Particle behavior in a Hall Thruster," AIAA-96-3195, 1996.
- ³⁴ Mikami, K., et al., "Optimization of Channel Configuration of Hall Thrusters," IEPC-95-33, 1995.
- ³⁵ Kusamoto, D. et al., "Exhaust beam profiles of Hall thrusters," ISTS-96-a-3, 1996.
- ³⁶ Komurasaki, K., et al., "Channel Length and Thruster Performance of Hall Thrusters," AIAA-96-3194, 1996
- ³⁷ Nakano, M. and Arakawa, Y., "Interplanetary trajectory optimization code for electric propulsion system study," AIAA-96-2981, 1996.